Electronic Supplementary Material (ESI) for Lab on a Chip.

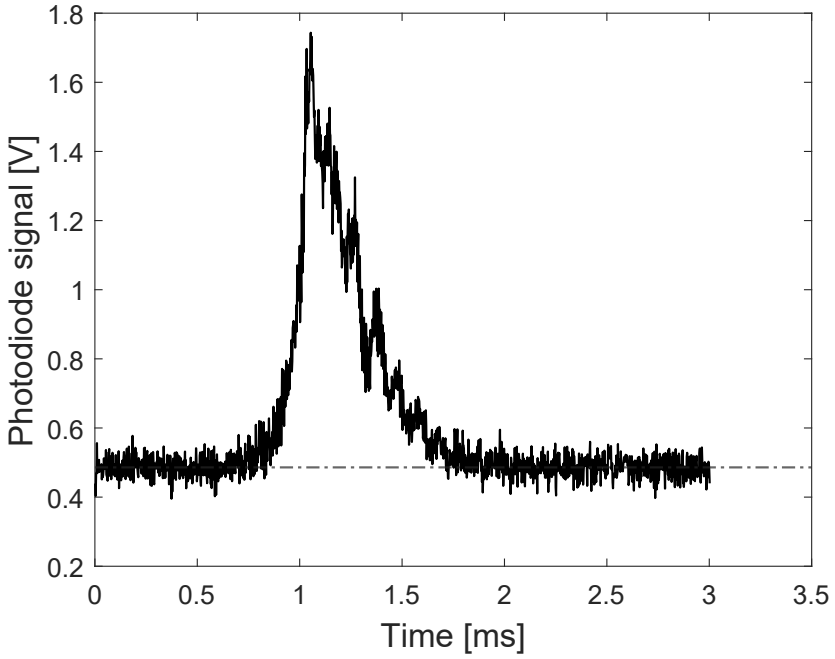

Figure 1 – Unfiltered angle-resolved signal. If the linearly variable OD filter is not used, the measured angle-resolved signal at high-angles is buried in the baseline noise. While it's still possible to compute the oscillation frequency in the time-domain and the signal integral, it's not possible to identify event start/end timepoints and the time-of-flight required to compute f_θ and to perform velocity compensation.

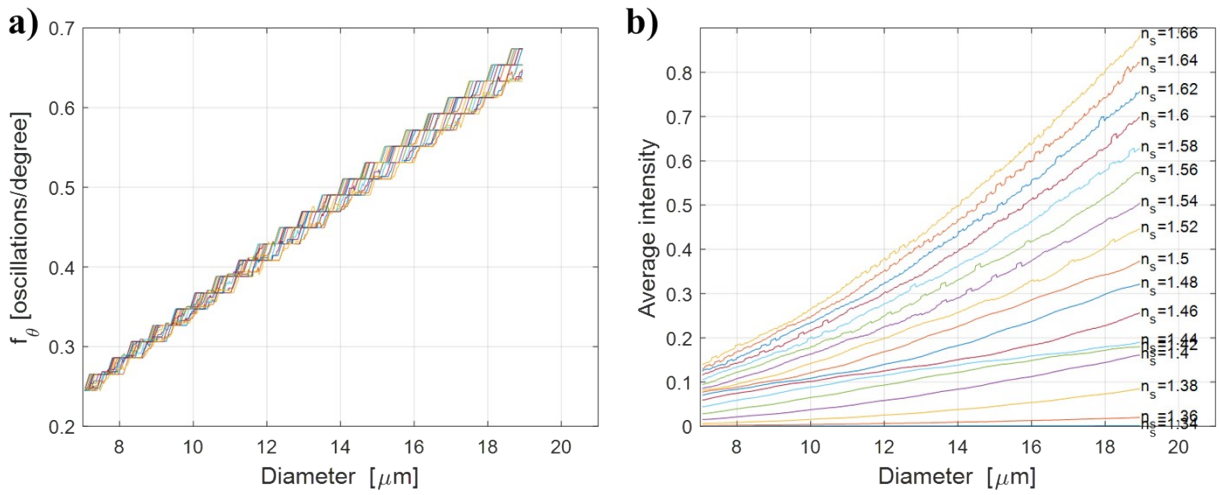

Figure 2 – Dependence of f_θ and average intensity from particle diameter and refractive index according to the Mie model. Each plot shows theoretical data for a single-shell sphere with different refractive index (n_s=1.34-1.66) over the 15°-65° angular range (n_m=1.335). **a)** f_θ depends only on particle diameter and is almost independent from its refractive index. **b)** The average intensity depends both on particle diameter and its refractive index. After computing the diameter using f_θ, the particle refractive index n_s is estimated using this look-up table.

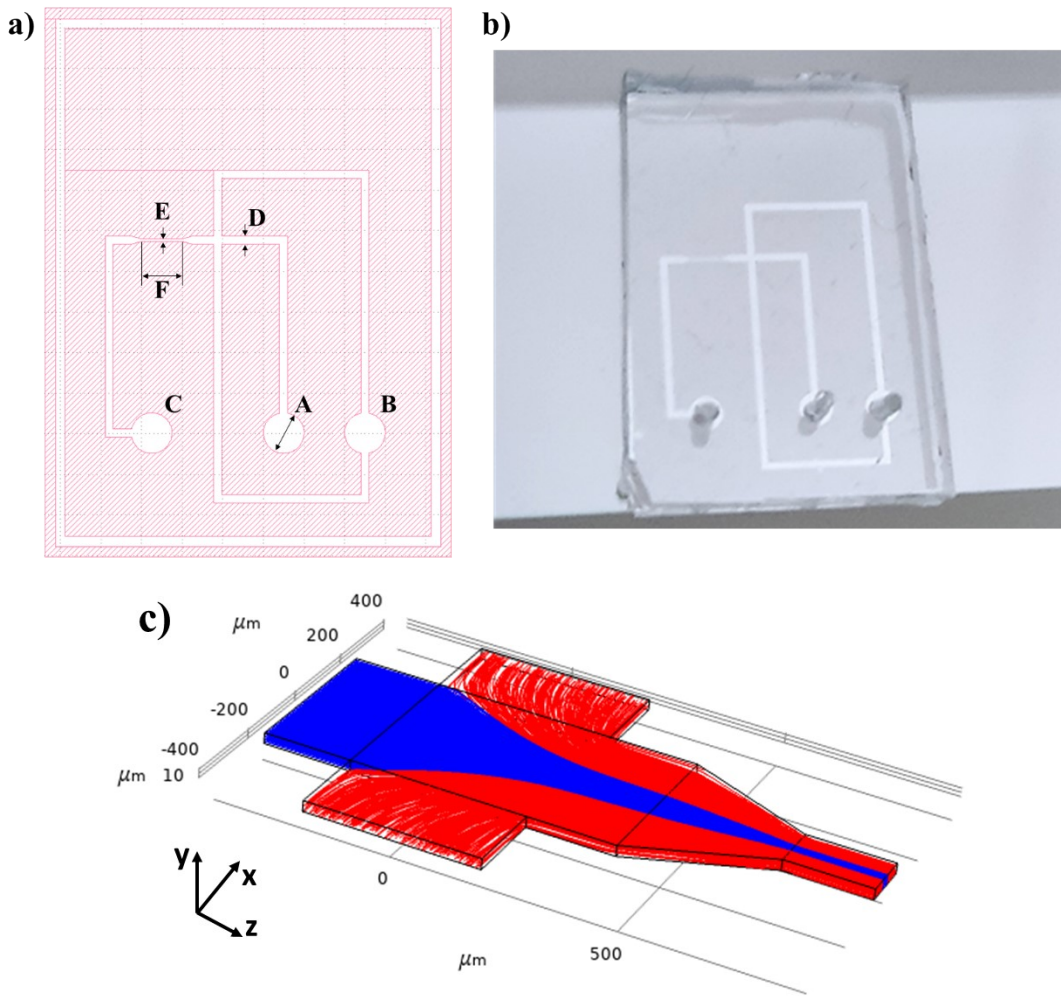

Figure 3 – Microfluidic chip. a) Schematic drawing: the microfluidic channels are formed by a sample channel and by two lateral sheath flow channels, which are designed to have the same hydraulic resistance and to focus the sample in the middle of the channel. The sample inlet (**a-A**), sheath flow inlet (**a-B**), and outlet (**a-C**) holes lie on a different line with respect to the measurement region to avoid interactions between the incoming laser beam and the tubing coming out of the chip. Channels width (**a-D**) is 400 μm everywhere with the exception of the measurement region (**a-E**) where it's 120 μm (**a-F**=2mm). The channel is 25 μm high. **b)** The PDMS chip is bonded to a glass slide after plasma exposure. **c)** Finite element analysis (FEA) of the flow focusing method used. The sample flow (blue streamlines) is focused by the sheath flows (red streamlines) towards the center of the microchannel along the x-axis, and occupies ≈30 μm after the channel narrowing.

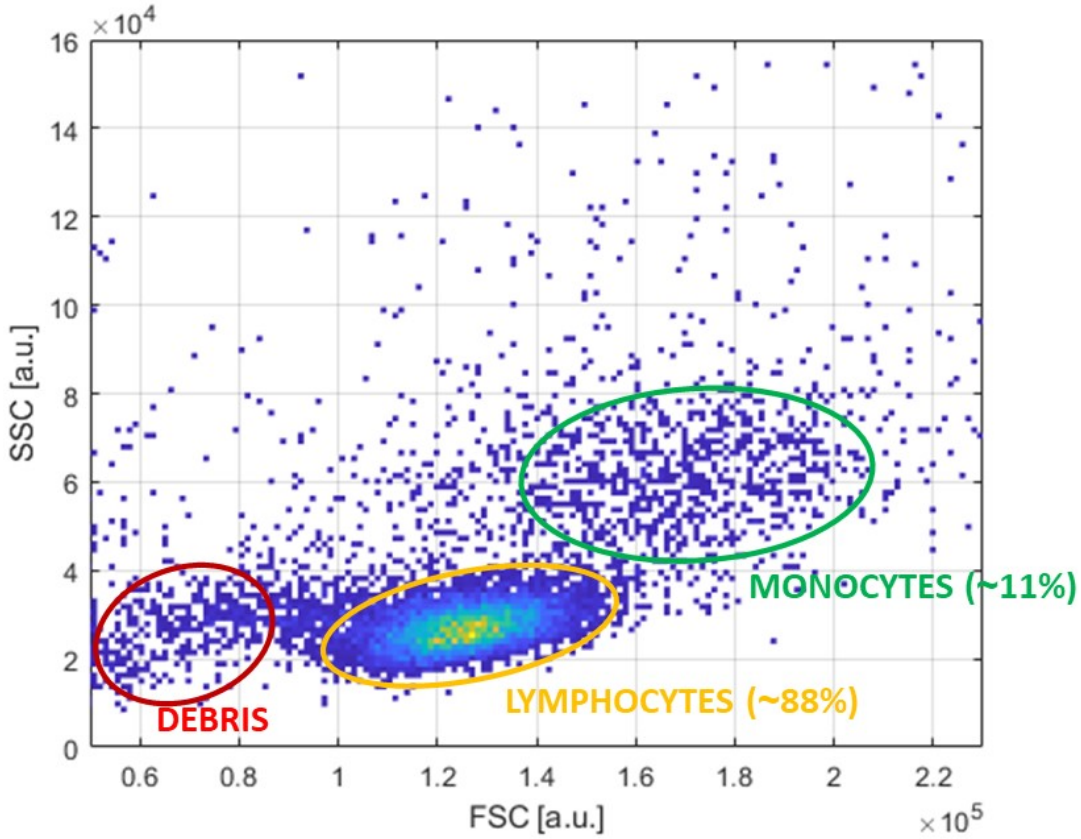

Figure 4 – FCM analysis of PBMC sample. The composition of the PBMC sample was verified using FCM and shown as a density plot. The sample was composed by lymphocytes (yellow, ~88%), monocytes (green ~11%), and debris (red).

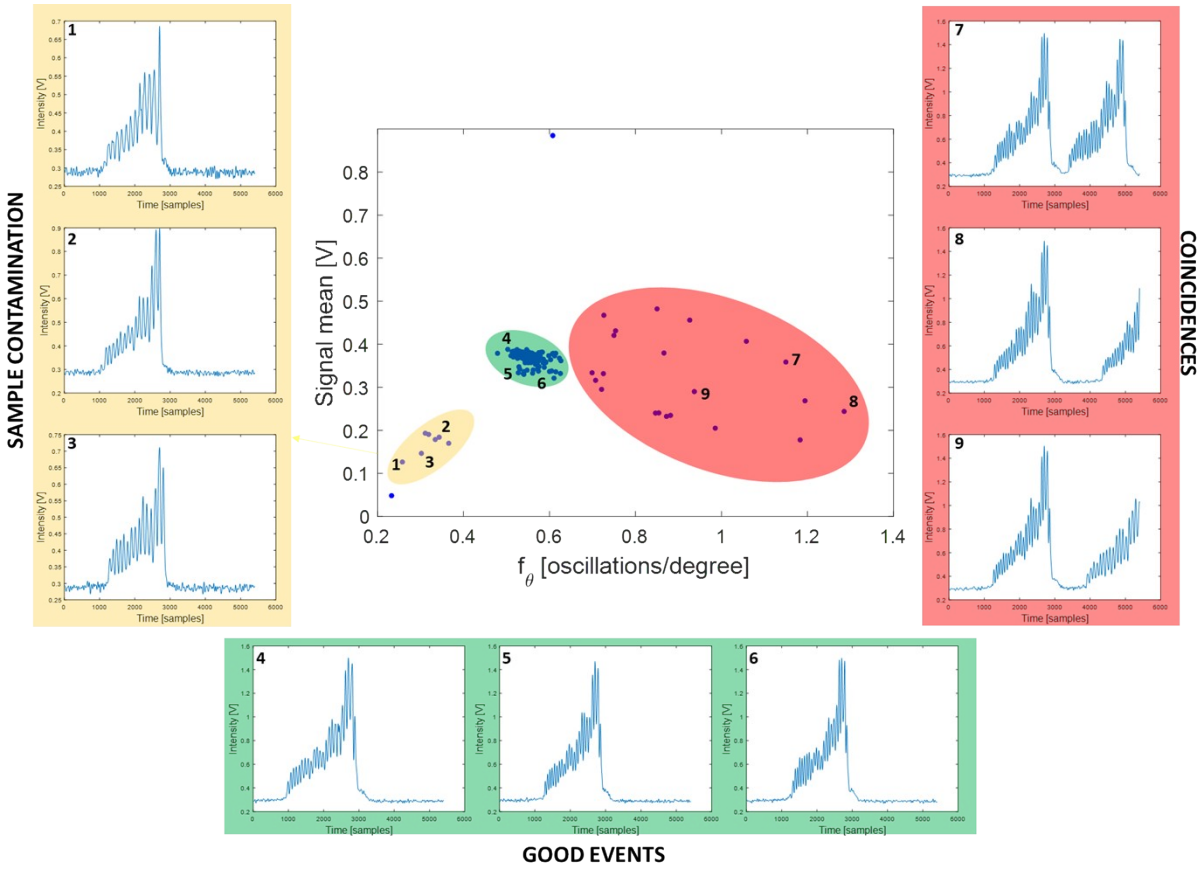

Figure 5 – Coincidence gating. A typical bivariate distribution obtained during an experiment is shown in the central scatter plot vs average intensity (relative to 15 μm PS beads). Three event subpopulations were identified, highlighted in green, yellow, and red. Each population was characterized by analyzing single events within it (selected events are shown in insets 1-9, the number show their position in the scatter plot): **1)** (Yellow region, insets 1-3): This population contains few events related to smaller beads, likely deriving from contamination with other samples. **2)** (Green region, insets 4-6): This population has the highest density and contains "good" events with single 15 mm beads. Only events within this region are considered for further analysis**. 3)** (Red region, insets 7-9): This population contains coincidences, i.e. events containing multiple 15 μm beads. Some events in this region aren't strictly multiple events, as the signals belonging to consecutive particles don't overlap. Nevertheless, they were discarded as they couldn't be reliably analyzed with current signal processing. Future efforts will be aimed at improving the signal processing algorithm to minimize such instances.

f_θ

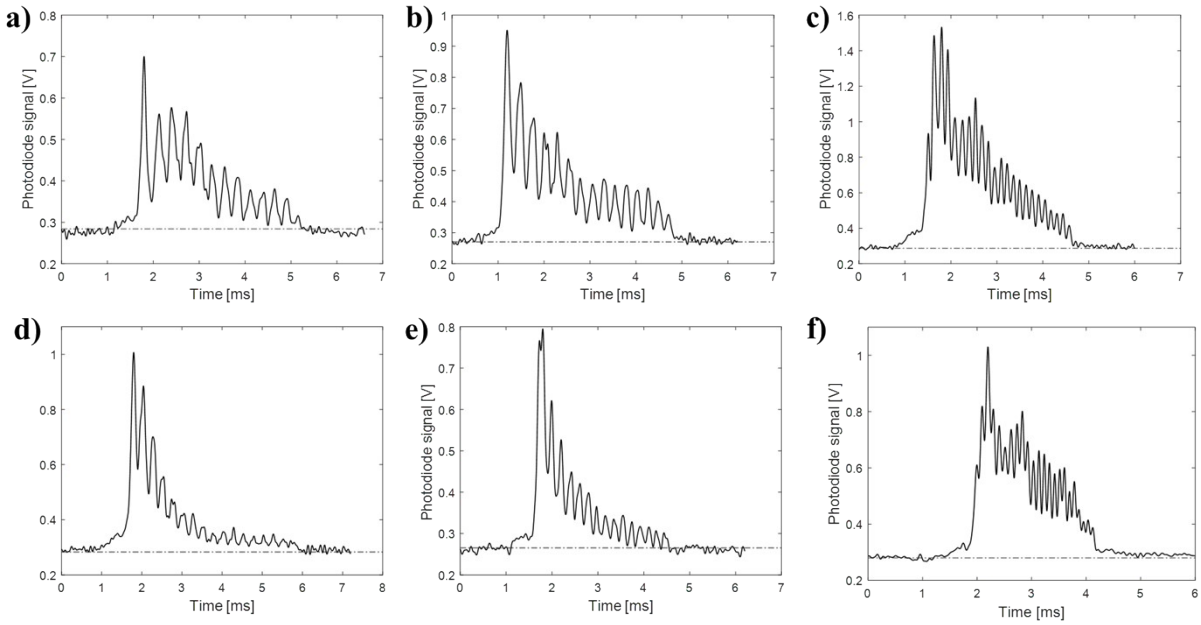

Figure 6 – Gallery of measured angle-resolved signals. Measured angle-resolved signals (after low-pass filtering to remove high frequency noise) representative of **a)** 9 μm PS beads, **b)** 10 μm PS beads, **c)** 15 μm PS beads, **d)** 10 μm SiO_2 beads, **e)** 10 μm PMMA beads, and **f)** monocytes.

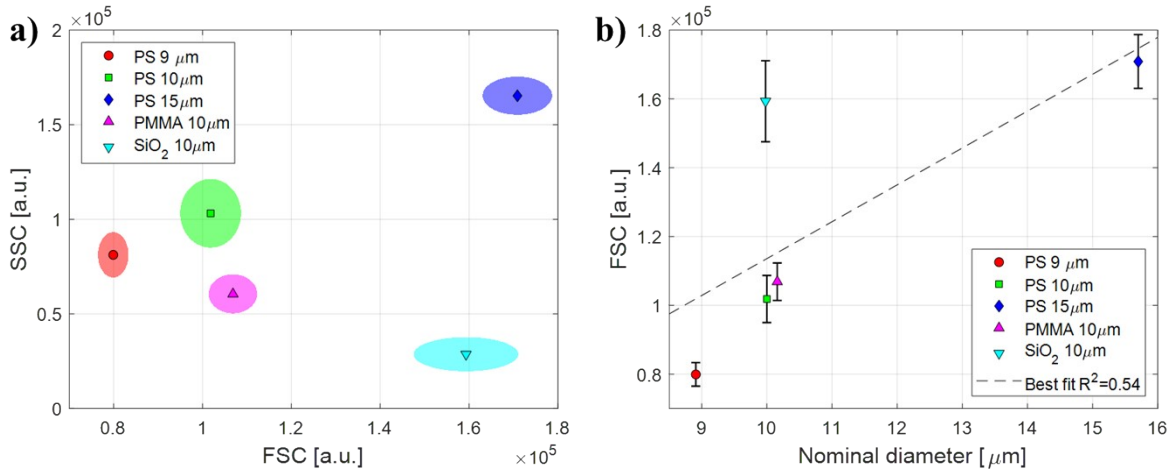

Figure 7 – FACS for size estimation. Polymeric beads with different sizes and refractive indices (Table 1 of main text) are used to assess the performance of FACS for size estimation. **a)** Data are shown as bivariate distributions (>200 events each) of FSC versus SSC. Markers represent distribution means, and shaded ellipses represent areas within one standard deviation of the mean. **b)** Linear regression of FSC with nominal beads diameter. Markers represent distribution means and error-bars represent one standard deviation. Black dashed line indicate the best-fit linear regression (R^2=0.54).